Figure of Merit of Polymer-Stabilized Blue Phase Liquid Crystals

Jin Yan, Yuan Chen, Shin-Tson Wu, *Fellow, IEEE*, and Xiaolong Song

***Abstract*—A figure of merit (FoM), defined as the ratio of Kerr constant to response time, is used to characterize and compare the electro-optic performance of polymer-stabilized blue phase liquid crystals (BPLCs). Increasing the dielectric anisotropy of LC host enhances Kerr constant and lowers the operation voltage, but its associated high viscosity dramatically increases the response time. As a result, the FoM may not be necessarily higher. For a given BPLC device, an optimal temperature exists where FoM reaches maximum. The proposed FoM provides useful guidelines for optimizing BPLCs for display and photonic applications.**

***Index Terms*—Blue phase, figure of merit (FoM), liquid crystals (LCs).**

I. Introduction

POLYMER-STABILIZED blue-phase liquid crystal (PS-BPLC) [1]–[3] is promising for display [4]–[6] and photonic [7], [8] applications because it exhibits following attractive features: alignment-layer free, microsecond response time [9], [10] and optically isotropic dark state. The electric field-induced birefringence can be described by extended Kerr effect [11]. The Kerr constant of PS-BPLC is 3–4 orders of magnitude larger than that of conventional Kerr media such as benzene, CS_2, water, nitrotoluene, and nitrobenzene [12], [13]. However, the Kerr constant of a PS-BPLC is still inadequate and the required operation voltage is still too high for active matrix addressing. To improve Kerr constant, much effort has been devoted to developing high dielectric anisotropy ($\Delta\varepsilon > 100$) LC hosts which in turn increases the viscosity and response time drastically [14], [15]. For such a large $\Delta\varepsilon$ LC host, the conventional capacitance measurement method would be inaccurate if the voltage shielding effect from the polyimide (PI) alignment layers is neglected. Moreover, the mean field theory [16] for describing the dielectric anisotropy has a presumption that $\Delta\varepsilon$ is small.

In this paper, we develop a method to characterize the high $\Delta\varepsilon$ LC hosts and propose a semi-empirical model to fit the experimental data. Good agreement is obtained. When $\Delta\varepsilon$ is small, our semi-empirical model is reduced to mean field theory. We then prepared four PS-BPLC samples using different $\Delta\varepsilon$ and viscosity materials. To compare their electro-optic performances, we define a figure of merit (FoM) as the ratio of Kerr constant to response time. Our results indicate that increasing $\Delta\varepsilon$ does not necessarily lead to a larger FoM; instead some side effects appear if $\Delta\varepsilon$ is too large. The FoM is also temperature dependent. For a given BPLC material, there is an optimal temperature where FoM has a maximum value.

TABLE I
PHYSICAL PARAMETERS OF THE FOUR LC HOSTS STUDIED AT ROOM TEMPERATURE AND $f = 1$ kHz. K AND τ ARE KERR CONSTANT AND RESPONSE TIME OF THE PSBP SAMPLES

Parameters	LC1	LC2	LC3	LC4
Δn	0.24	0.16	0.2	0.17
$\Delta\varepsilon$	13.76	56.71	95.53	251.41
γ_1 ($pa{\cdot}s$)	0.35	0.45	0.40	2.14
K (nm/V^2)	0.43	1.07	2.65	3.71
τ (ms)	0.107	0.114	0.119	0.347

II. Experiment

First, we studied four different nematic LC hosts with different dielectric anisotropies designated as LC 1–4. Table I lists the measured Δn, $\Delta\varepsilon$ and γ_1 of the four LC hosts at room temperature ($\sim 22°$C) and $f = 1$ kHz driving frequency. The dielectric anisotropies are measured using a LCR meter (HIORI LCR HiTESTER 3532-50). Homogenously aligned cells are used when we measure $\varepsilon_\perp$ and vertically aligned cells are employed while measuring $\varepsilon_{//}$. Special caution has to be taken when characterizing a large $\Delta\varepsilon$ LC. Since a LC cell can be treated as three capacitors [one LC layer and two ultrathin PI layers] in series [17], the measured dielectric constant ε is derived as

$$\varepsilon = \frac{1}{\frac{\frac{2d_p}{d}}{\varepsilon_p} + \frac{1-\frac{2d_p}{d}}{\varepsilon_{\rm LC}}} \tag{1}$$

where d is the cell gap, d_p and ε_p are the *effective* thickness and dielectric constant of the PI layer, and $\varepsilon_{\rm LC}$ is the dielectric constant ($\varepsilon_{//}$ or $\varepsilon_\perp$) of the LC host. If $\varepsilon_{\rm LC}$ is comparable to ε_p (~ 3), the first term in the denominator can be neglected since $d_p \ll d$ so that $\varepsilon \approx \varepsilon_{\rm LC}$. For a strong polar LC, its $\varepsilon_{//}$ is very large so that the capacitance of the PI layers cannot be ignored. For example, let us assume $\varepsilon_{\rm LC} = 200$, $d = 8$ μm, and $d_p = 30$ nm (the deposited PI layer thickness is ~ 80 nm,

Manuscript received August 06, 2012; accepted September 26, 2012. Date of publication November 19, 2012; date of current version January 14, 2013. This work was supported by Industrial Technology Research Institute (ITRI, Taiwan).

J. Yan, Y. Chen, and S.-T. Wu are with the College of Optics and Photonics, University of Central Florida, Orlando, FL 32816 USA (e-mail: jyan@creol.ucf.edu; yuanucf@knights.ucf.edu; swu@mail.ucf.edu).

X. Song is with Jiangsu Hecheng Display Technology Company, Nanjing 210014, China (email: song@hcch.net.cn).

Color versions of one or more of the figures are available online at http://ieeexplore.ieee.org.

Digital Object Identifier 10.1109/JDT.2012.2222015

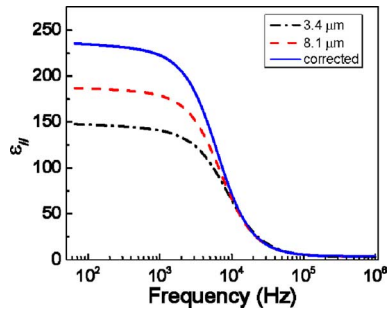

Fig. 1. Measured $\varepsilon_{//}$ of LC4 at 30°C using two cells with 3.4 μm and 8.1 μm cell gaps, and corrected $\varepsilon_{//}$ according to (2).

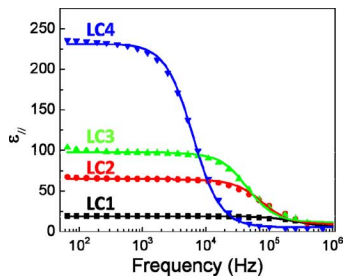

Fig. 2. Frequency dependent $\varepsilon_{//}$ of four LCs at 30 °C. Dots are corrected experimental data and lines are fitting with (3).

but the rubbing process would reduce its effective thickness), the obtained ε from (1) is only 134. The discrepancy is as large as 33%. Therefore, the measured value is often smaller than it should be because of the shielding effect from the PI layers.

Fig. 1 shows the measured $\varepsilon_{//}$ of LC4 at 30 °C using two cells with different cell gaps d_1 and d_2. The $\varepsilon_{\perp}$ of a LC is usually small so the PI effect can be neglected. Since LC4 has a very large $\varepsilon_{//}$, the PI effect should be taken into account for the measurement of $\varepsilon_{//}$. For different cell gaps, the measured $\varepsilon_{//}$ are different because of the different d_p/d in (1), as shown in Fig. 1. Therefore, the measured value needs to be corrected in order to obtain the real value of $\varepsilon_{//}$. Assuming the PI layers in the two cells have the same thickness d_p, we obtain the corrected expression for $\varepsilon_{//}$ after some algebra

$$\varepsilon_{//} = \frac{d_1 - d_2}{\frac{d_1}{\varepsilon_1} - \frac{d_2}{\varepsilon_2}} \tag{2}$$

where ε_1 and ε_2 are the measured values using these two cells. The corrected $\varepsilon_{//}$ is plotted in Fig. 1. The values shown in Table I are also corrected.

Fig. 2 shows the dielectric relaxation of $\varepsilon_{//}$ for the four LC hosts at 30 °C. $\varepsilon_{\perp}$ is almost a constant (not shown here) in the entire plotted region. The data are fitted using Debye relaxation equation

$$\varepsilon_{//} = \varepsilon_{\infty} + \frac{\varepsilon_0 - \varepsilon_{\infty}}{1 + \left(\frac{f}{f_r}\right)^2} \tag{3}$$

where ε_0 is the static permittivity at low frequency, ε_{∞} is the permittivity at the high frequency limit, and f_r is the relaxation frequency. The fitting parameters ε_0, ε_{∞}, and f_r are listed in Table II. From Table II, we find that a larger $\Delta\varepsilon$ LC has a lower relaxation frequency as expected. Generally speaking, a larger $\Delta\varepsilon$ LC consists of more polar groups and therefore it is more bulky and viscous. So it is more difficult for the molecules to follow the electric field, which results in a lower relaxation frequency. A low relaxation frequency implies that the Kerr constant decreases sharply as the electric field frequency approaches f_r [18]. This could be problematic for high frequency (say, a few kHz) operation of BPLC devices.

TABLE II
FITTING PARAMETERS FOR THE FOUR LC HOSTS AT 30 °C

Parameters	LC1	LC2	LC3	LC4
ε_0	19.02	64.58	97.53	231.45
ε_∞	5.63	8.98	11.72	5.47
f_r (kHz)	278.3	75.7	44.7	6.2

Next, we prepared four PS-BPLC samples using the four LC hosts. The BPLC precursors consist of a LC host, a chiral dopant (R5011, HCCH), 10 wt% monomers [6% RM257 (Merck) and 4% TMPTA (1,1,1-Trimethylolpropane Triacrylate, Sigma Aldrich)] [19], and a small amount ($\sim$ 0.6%) of photoinitiator. Since the helical twist power of chiral dopant changes in different LC hosts, the concentration of the chiral dopant varies from 4.5% to 7% in order to obtain similar pitch length. The four precursors were cured by UV light with an intensity of 2 mW/cm^2 for 30 min near the transition temperature from chiral nematic phase to blue phase. We used vertical-field switching (VFS) cells [20], [21] instead of in-plane-switching (IPS) cells because an uniform electric field is preferable to characterize the electro-optic performance of PS-BPLC materials.

III. RESULTS AND DISCUSSION

From Gerber's model [22], the Kerr constant (K) of a BPLC can be approximated as

$$K \sim \frac{\Delta n_{\mathrm{ind}}}{\lambda E^2} \approx \Delta n \cdot \Delta\varepsilon \frac{\varepsilon_o P^2}{k\lambda(2\pi)^2} \tag{4}$$

and the response time can be estimated by

$$\tau \approx \frac{\gamma_1 P^2}{k(2\pi)^2} \tag{5}$$

where Δn_{ind} is the induced birefringence, λ is the wavelength, Δn is the intrinsic birefringence of LC host, k is the averaged elastic constant which is affected by both LC host and polymer network, P is the pitch length, and γ_1 is the rotational viscosity of the LC host. The viscosity of BPLC composite will increase after adding chiral dopants; here we assume the viscosity of BPLC is proportional to that of the LC host, provided that the same chiral dopant and similar pitch length are obtained. Δn, $\Delta\varepsilon$ and γ_1 can be obtained from the LC host and pitch length can be measured from the reflection spectrum of the PS-BPLC. However, the averaged elastic constant is difficult to identify. Moreover, Kerr constant and response time have contradicting requirements. For example, a longer pitch length and a smaller elastic constant are favorable for enhancing Kerr constant, but

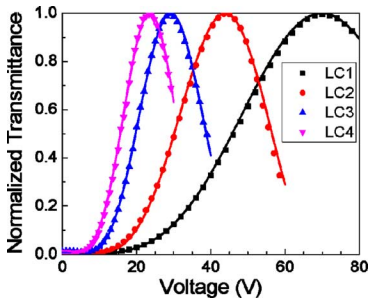

Fig. 3. Measured VT (dots) of PS-BPLCs at room temperature and 1 kHz frequency and fitting (lines) using extended Kerr effect model. $\theta = 70°$.

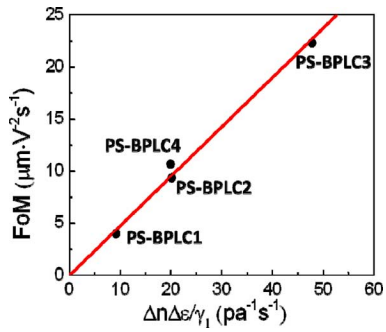

Fig. 4. FoM of four PS-BPLCs using VFS cells. Red line is linear fitting with (6).

unfavorable for response time. Therefore, we define a figure of merit (FoM) as

$$\mathrm{FoM} = \frac{K}{\tau} \propto \frac{\Delta n \Delta \varepsilon}{\gamma_1} \tag{6}$$

for comparing and optimizing the BPLC performance at a given wavelength and pitch length. A large Kerr constant and a fast response time would lead to a high FoM.

Fig. 3 depicts the measured voltage-dependent transmittance (VT) curves of the four VFS cells. The measurement method has been reported in [20]. Here, the light incident angle is 70°. The experimental data are fitted by a simulation program incorporating extended Kerr effect model [11]. Table I lists the obtained Kerr constants. Response time is also measured and results are included in the bottom row of Table I. While measuring response time, we remove the voltage instantaneously from V_p which corresponds to the peak transmittance. Response time is defined as the transmittance change from 90% to 10%. Although the optical decay time is different from the phase decay time [23], it is proportional to the phase decay time for the same grayscale operation.

In Fig. 3, theoretically there is no threshold for the VT curves because the induced birefringence can be expressed as [11]

$$\Delta n_{\mathrm{ind}} = \Delta n_{\mathrm{sat}} \left(1 - \exp\left[-\left(\frac{E}{E_s} \right)^2 \right] \right) \tag{7}$$

where Δn_{sat} stands for the saturated induced birefringence and E_S represents the saturation field. In (7), the induced birefringence increases with the electric field. The threshold-like behavior in Fig. 3 is because the transmittance is related to the phase retardation δ by a sinusoidal equation as

$$T = \sin^2\left(\frac{\delta}{2} \right). \tag{8}$$

Details about the induced phase retardation have been discussed in [23]. With amorphous silicon thin-film-transistor (TFT) addressing, the fluctuation voltage (V_f) could reach 0.5–0.8 V. For an LC device without a threshold voltage, the dark state could be degraded. Although BPLC has no threshold voltage, the threshold-like performance provides a good dark state. Let us assume the on-state voltage is $\sim$ 10 V. Through simulation we found that a contrast ratio over 1000:1 can be achieved if $V_f < 1.3$ V.

Fig. 4 shows the linear relationship between FoM and $\Delta n \Delta \varepsilon / \gamma_1$ of the LC host. Good agreement between experimental data and linear fitting is obtained. The slope will be affected by the type and concentration of monomer and chiral agent employed, and also device structures. For the four PS-BPLC samples, we used same amount of monomer and similar pitch length, so the slope is similar for the four BPLC samples. From Fig. 4, by increasing the dielectric anisotropy of the LC hosts, FoM first increases due to the improved Kerr constant. However, the improvement on Kerr constant gradually saturates when $\Delta\varepsilon > 100$, but in the meantime viscosity increases dramatically so that the response time slows down. As a result, PS-BPLC4 has a smaller FoM than PS-BPLC3. Moreover, LC4 has a low relaxation frequency which will cause a strong frequency dependency on Kerr constant and also dielectric heating, which are undesirable for display applications. PS-BPLC3 exhibits the highest FoM among the four samples studied; it has a good balance between Kerr constant and response time.

One question that arises is the voltage shielding effect from the polymer network because $\sim$ 10 wt% polymer is employed. However, the polymer network in BPLC is uniformly distributed in the composites, instead of being separated from the LC layer (such as PI layers), so the polymer is not only in series but also in parallel with the BPLC composite. We have attempted to estimate the voltage shielding effect from the polymer microscopically and found that it is not too significant. In terms of applications, the macroscopic performance is the major concern. Here, we treat the PS-BPLC system as a whole; the Kerr constant is a macroscopic parameter obtained from the experimentally measured VT curves.

FoM is temperature dependent since Δn, $\Delta\varepsilon$ and γ_1 are all temperature sensitive. The temperature dependency of Δn and γ_1 is described as follows [24]–[26]:

$$\Delta n = \Delta n_0 S \tag{9}$$

$$\gamma_1 = aS \exp\left(\frac{E}{k_B T} \right) \tag{10}$$

where S is the order parameter, Δn_0 is the extrapolated birefringence at $T = 0\ K$, E is the activation energy, k_B is the Boltzmann constant, and a is a proportionality constant. The order parameter S can be approximated well by Haller's equation [27], [28]

$$S = \left(1 - \frac{T}{T_c} \right)^{\beta} \tag{11}$$

TABLE III
FITTING PARAMETERS FOR LC3 AND LC4

Parameters	LC3	LC4
T_c (°C)	96	75.5
β	0.225	0.205
E (meV)	478	762
U (meV)	123	276
b	1.13	0.0086

where T_c stands for the nematic-isotropic phase transition temperature of a LC and β is a material constant. The order parameters are determined from the temperature dependent birefringence. The activation energy in (10) can be obtained from the measured temperature dependent visco-elastic constant of the LC host using anti-parallel rubbed cells. The obtained β and E for the LC3 and LC4 are listed in Table III.

From Maier and Meier's mean field theory [16], $\Delta\varepsilon$ is proportional to S/T. But in the derivation of mean field theory, an approximation that $\Delta\varepsilon \ll \bar{\varepsilon}$ ($\bar{\varepsilon}$ is the averaged dielectric constant) was made so that the local fields are treated as isotropic. However, for LCs with a large dielectric anisotropy, the local field effect would be much stronger and cannot be taken as isotropic. Therefore, mean field theory is no longer valid for large $\Delta\varepsilon$ materials.

Fig. 5 depicts the measured temperature dependent dielectric constants of LC3 and LC4. All the data are taken at low frequencies before the dielectric relaxation occurs and corrected according to (2). From Fig. 5, $\Delta\varepsilon$ has a strong temperature dependency which mainly comes from $\varepsilon_{//}$, while $\varepsilon_{\perp}$ does not change much with the temperature. Since it is very difficult to address the anisotropy of local fields, here we propose an empirical equation for describing the temperature dependency of large $\Delta\varepsilon$ LCs

$$\Delta\varepsilon = b \cdot S \exp\left(\frac{U}{k_B T}\right) \tag{12}$$

where U is a parameter related to the dipole moment and b is a proportionality constant. The order parameter can be determined from the temperature dependent birefringence, so there are only two adjustable parameters in (12): U and b. The fittings with experimental data are very good for both LC hosts. The two fitting parameters are also included in Table III.

It is interesting to note that when the dipole moment is small (i.e., $U \ll k_B T$), the exponential term can be expanded as $\exp(U/k_B T) \ll 1 + U/k_B T$ and (12) is reduced to

$$\Delta\varepsilon = b \cdot S\left(1 + \frac{U}{k_B T}\right). \tag{13}$$

Equation (13) has the same form as mean field theory. Therefore, (12) is applicable for both large and small $\Delta\varepsilon$ LC materials. Although it seems (12) tends to be divergent at low temperature, the relaxation frequency also shifts to a lower frequency as the temperature decreases. Equation (12) will not be valid if $\Delta\varepsilon$ starts to relax at the measurement frequency.

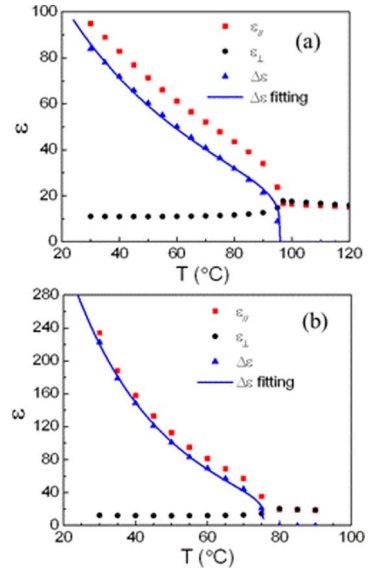

Fig. 5. Measured $\varepsilon_{//}$, $\varepsilon_{\perp}$, and $\Delta\varepsilon$ (dots) of: (a) LC3 and (b) LC4, and fittings (lines) using (12).

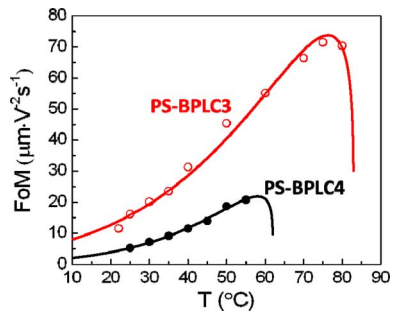

Fig. 6. Temperature dependent FoM for two PS-BPLCs using IPS cells and fittings (lines) with (14).

Combining (9), (10), and (12), the temperature dependency of FoM is derived as

$$\mathrm{FoM} = cS \exp\left[\frac{(U-E)}{k_B T}\right] \tag{14}$$

where c is a proportionality constant. For a polymer-stabilized BPLC, the clearing temperature T_{c_BP} is often few degrees lower than that of the LC host after adding chiral dopant. As a result, the order parameter S is slightly different from that of the LC host, by substituting T_c with T_{c_BP}. To verify (14), we prepared two PS-BPLC cells using LC3 and LC4. Here IPS cells with electrode width $w = 10$ μm and electrode gap $g = 10$ μm are employed because it is difficult to control the temperature of a VFS cell. The FoM for an IPS cell is somewhat different from a VFS cell because their Kerr constant and response time are different. The response time difference is due to the nonuniform electric field distribution in the IPS cell [20], while the reason for the Kerr constant difference is still under investigation. In spite of different FoM, the temperature dependency of IPS cells should still roughly follow (14).

Fig. 6 shows the FoM of the two IPS cells. The Kerr constants are obtained by fitting the VT curves using a simulation program [29] which has taken the nonuniform electric field into account. The response time is also defined as 90%–10% transmittance

change. The data are fitted with (14) with only one adjustable parameter c. Other parameters U, E and β are obtained from LC hosts, and T_{c_BP} is measured using a polarized optical microscope. The fittings with (14) are very good for both cells, which indicates that the temperature dependent FoM is basically determined by the LC host, while the polymer and chiral will only affect the adjustable parameter c. For a given PSBP, an optimal temperature (T_{op}) exists which gives the maximum FoM [30]. This can be understood qualitatively as follows: as the temperature increases, Kerr constant decreases mainly due to the reduced $\Delta\varepsilon$, but the decreasing rate in Kerr constant is slower than that of response time, resulting in an increased FoM. As the temperature gets closer to T_c, Kerr constant decreases dramatically which leads to a sharp decrease in FoM. To derive the optimal temperature, we set $d(FoM)/dT = 0$ and find

$$T_{\mathrm{op}} = T_c - \frac{\beta k_B T_c^2}{E - U}. \tag{15}$$

Substituting (15) with the parameters of PS-BPLC3, we found the optimal temperature is $\sim 7\,^{\circ}\mathrm{C}$ below T_c. At the optimal temperature, maximum FoM is achieved mainly because of the fast response time, but the Kerr constant is fairly small which demands a high driving voltage. For some photonics applications which require fast response time while the driving voltage is less concerned, the device can be operated at this optimal temperature. Material systems can also be optimized to achieve maximum FoM at room temperature.

IV. Conclusion

In conclusion, we defined a FoM to characterize and compare the performance of PS-BPLC materials. FoM is closely related to the properties of host LCs. Good agreement between experimental results and theory is obtained. Although increasing the $\Delta\varepsilon$ of a LC host enhances Kerr constant which is favorable for reducing voltage, these strong polar materials also increase the viscosity and response time dramatically. As a result, the overall FoM may not gain. For a given material, there is an optimal temperature for achieving maximum FoM. We also found that conventional method needs correction for measuring the dielectric constants of large $\Delta\varepsilon$ LC materials. Moreover, mean field theory is no longer valid for large $\Delta\varepsilon$ LCs and an empirical equation was proposed to illustrate the divergence behavior of $\Delta\varepsilon$ at low temperature. Again, the proposed model fits well with experimental results. This study will make a significant impact on both LC materials and BPLC materials characterization and optimization.

References

[1] H. Kikuchi, M. Yokota, Y. Hisakado, H. Yang, and T. Kajiyama, "Polymer-stabilized liquid crystal blue phases," *Nat. Mater.*, vol. 1, pp. 64–68, 2002.

[2] Y. Hisakado, H. Kikuchi, T. Nagamura, and T. Kajiyama, "Large electro-optic Kerr effect in polymer-stabilized liquid crystalline blue phases," *Adv. Mater.*, vol. 17, pp. 96–98, 2005.

[3] J. Yan, L. Rao, M. Jiao, Y. Li, H. C. Cheng, and S. T. Wu, "Polymer-stabilized optically isotropic liquid crystals for next-generation display and photonics applications," *J. Mater. Chem.*, vol. 21, pp. 7870–7877, 2011.

[4] Z. Ge, S. Gauza, M. Jiao, H. Xianyu, and S. T. Wu, "Electro-optics of polymer-stabilized blue phase liquid crystal displays," *Appl. Phys. Lett.*, vol. 94, p. 101104, 2009.

[5] L. Rao, Z. Ge, S. T. Wu, and S. H. Lee, "Low voltage blue-phase liquid crystal displays," *Appl. Phys. Lett.*, vol. 95, p. 231101, 2009.

[6] M. Jiao, Y. Li, and S. T. Wu, "Low voltage and high transmittance blue-phase liquid crystal displays with corrugated electrodes," *Appl. Phys. Lett.*, vol. 96, p. 011102, 2010.

[7] J. Yan, Y. Li, and S. T. Wu, "High-efficiency and fast-response tunable phase grating using a blue phase liquid crystal," *Opt. Lett.*, vol. 36, p. 1404, 2011.

[8] Y. H. Lin, H. S. Chen, H. C. Lin, Y. S. Tsou, H. K. Hsu, and W. Y. Li, "Polarizer-free and fast response microlens arrays using polymer-stabilized blue phase liquid crystals," *Appl. Phys. Lett.*, vol. 96, p. 113505, 2010.

[9] K. M. Chen, S. Gauza, H. Xianyu, and S. T. Wu, "Submillisecond gray-level response time of a polymer-stabilized blue-phase liquid crystal," *J. Display Technol.*, vol. 6, no. 2, pp. 49–51, Feb. 2010.

[10] Y. Chen, J. Yan, J. Sun, S. T. Wu, X. Liang, S. H. Liu, P. J. Hsieh, K. L. Cheng, and J. W. Shiu, "A microsecond- response polymer-stabilized blue phase liquid crystal," *Appl. Phys. Lett.*, vol. 99, p. 201105, 2011.

[11] J. Yan, H. C. Cheng, S. Gauza, Y. Li, M. Jiao, L. Rao, and S. T. Wu, "Extended Kerr effect of polymer-stabilized blue-phase liquid crystals," *Appl. Phys. Lett.*, vol. 96, p. 071105, 2010.

[12] J. W. Beams, "Electric and magnetic double refraction," *Rev. Mod. Phys.*, vol. 4, pp. 133–172, 1932.

[13] M. Jiao, J. Yan, and S. T. Wu, "Dispersion relation on the Kerr constant of a polymer-stabilized optically isotropic liquid crystal," *Phys. Rev. E*, vol. 83, p. 041706, 2011.

[14] L. Rao, J. Yan, S. T. Wu, S. Yamamoto, and Y. Haseba, "A large Kerr constant polymer-stabilized blue phase liquid crystal," *Appl. Phys. Lett.*, vol. 98, p. 081109, 2011.

[15] M. Wittek, N. Tanaka, D. Wilkes, M. Bremer, D. Pauluth, J. Canisius, A. Yeh, R. Yan, K. Skjonnemand, and M. K. Memmer, "New materials for polymer-stabilized blue phase," in *SID Int. Symp. Dig. Tech. Papers*, 2012, vol. 43, pp. 25–28.

[16] W. Maier and G. Meier, "A simple theory of the dielectric characteristics of homogeneous oriented crystalline-liquid phases of the nematic type," *Z. Naturf. A*, vol. 16, pp. 262–267, 1961.

[17] M. Jiao, Z. Ge, Q. Song, and S. T. Wu, "Alignment layer effects on thin liquid crystal cells," *Appl. Phys. Lett.*, vol. 92, p. 061102, 2008.

[18] Y. Li, Y. Chen, J. Sun, S. T. Wu, S. H. Liu, P. J. Hsieh, K. L. Cheng, and J. W. Shiu, "Dielectric dispersion on the Kerr constant of blue phase liquid crystals," *Appl. Phys. Lett.*, vol. 99, p. 181126, 2011.

[19] J. Yan and S. T. Wu, "Polymer-stabilized blue phase liquid crystals: A tutorial," *Opt. Mater. Express*, vol. 1, pp. 1527–1535, 2011.

[20] H. C. Cheng, J. Yan, T. Ishinabe, and S. T. Wu, "Vertical field switching for blue-phase liquid crystal devices," *Appl. Phys. Lett.*, vol. 98, p. 261102, 2011.

[21] H. C. Cheng, J. Yan, T. Ishinabe, N. Sugiura, C. Y. Liu, T. H. Huang, C. Y. Tsai, C. H. Lin, and S. T. Wu, "Blue-phase liquid crystal displays with vertical field switching," *J. Display Technol.*, vol. 8, no. 2, pp. 98–103, 2012.

[22] P. R. Gerber, "Electro-optical effects of a small-pitch blue-phase system," *Mol. Cryst. Liq. Cryst.*, vol. 116, pp. 197–206, 1985.

[23] J. Yan, Y. Chen, S. T. Wu, S. H. Liu, K. L. Cheng, and J. W. Shiu, "Dynamic response of a polymer-stabilized blue-phase liquid crystal," *J. Appl. Phys.*, vol. 111, p. 063103, 2012.

[24] E. M. Averyanov and V. F. Shabanov, "Structural and optical anisotropy of liquid crystals," *Sov. Phys. Crystallogr.*, vol. 23, p. 177, 1978.

[25] S. T. Wu, "Birefringence dispersions of liquid crystals," *Phys. Rev. A*, vol. 33, pp. 1270–1274, 1986.

[26] V. V. Belyaev, S. A. Ivanov, and M. F. Gorebenkin, "Temperature dependence of rotational viscosity of nematic liquid crystals," *Sov. Phys. Crystallogr.*, vol. 30, p. 674, 1985.

[27] I. Haller, "Thermodynamic and static properties of liquid crystals," *Prog. Solid State Chem.*, vol. 10, pp. 103–118, 1975.

[28] A. Saupe, "Temperature dependence and magnitude of deformation constants in strained liquids," *Z. Naturforsch. Teil A*, vol. 15, pp. 810–814, 1960.

[29] Z. Ge, L. Rao, S. Gauza, and S. T. Wu, "Modeling of blue phase liquid crystal displays," *J. Display Technol.*, vol. 5, no. 7, pp. 250–256, Jul. 2009.

[30] S. T. Wu, A. M. Lackner, and U. Efron, "Optimal operation temperature of liquid crystal modulators," *Appl. Opt.*, vol. 26, pp. 3441–3445, 1987.

Jin Yan is currently working toward the Ph.D. degree from the College of Optics and Photonics, University of Central Florida.

Her research interests include device physics and materials of polymer-stabilized blue phase and isotropic phase liquid crystal displays. She has 19 journal publications.

Ms. Yan is a recipient of a 2012 SPIE scholarship and 2012 IEEE graduate student fellowship award.

Yuan Chen received the B.S. degree in information engineering from Zhejiang University, China, in 2007, and is currently working toward the Ph.D. degree from the College of Optics and Photonics, University of Central Florida, Orlando.

Her current research interests include novel organic materials and devices for advanced display and photonic applications, and low loss infrared liquid crystals. She has 13 journal publications.

Shin-Tson Wu (M'98–SM'99–F'04) received the B.S. degree in physics from National Taiwan University, and the Ph.D. degree from the University of Southern California, Los Angeles.

He is a Pegasus professor at College of Optics and Photonics, University of Central Florida, Orlando.

Dr.Wu is the recipient of 2011 SID Slottow-Owaki prize, 2010 OSA Joseph Fraunhofer award, 2008 SPIE G. G. Stokes award, and 2008 SID Jan Rajchman prize. He was the founding Editor-in-Chief of IEEE/OSA JOURNAL OF DISPLAY TECHNOLOGY. He is a Fellow of the Society of Information Display (SID), Optical Society of America (OSA), and SPIE.

Xiaolong Song, photograph and biography not available at time of publication.